

Sensitivities of SCMs to New Parameterizations of Cloud-Radiative Interactions

G. M. McFarquhar
Department of Atmospheric Sciences
University of Illinois,
Urbana, Illinois

S. F. Iacobellis and R. C. J. Somerville
Scripps Institution of Oceanography
La Jolla, California

G. G. Mace and Y. Zhang
Department of Atmospheric Sciences
University of Utah
Salt Lake City, Utah

Introduction

Accurate parameterizations of, and in terms of, ice cloud effective radius (r_e) are crucial for accurate model estimates of upwelling and downwelling radiative fluxes, and of cloud radiative forcing (CRF). Zhang et al. (1999), and Iacobellis and Somerville (2000) have all found that radiative fluxes are sensitive to the specification of r_e and fallout, and that the most realistic vertical distribution of clouds is obtained from model simulations that include the most complete representation of cloud microphysics.

Based on in situ observations of the sizes of ice crystals obtained in blowoff anvils in the Tropics during the Central Equatorial Pacific Experiment (McFarquhar and Heymsfield 1997), and on estimates of ice crystal shape derived from a neural network (McFarquhar et al. 1999), a new bulk parameterization of the dependence of r_e on ice water content (IWC) and temperature is derived. The parameterization includes uncertainty estimates so that sensitivities of model parameters to possible variations in r_e can be computed. The in situ data used to develop the parameterization are, supplemented with cirrus layer microphysical properties retrieved from surface-based millimeter wave cloud radar (MMCR) and atmospheric emitted radiance interferometer (AERI) data, for the June and July 1999 time period at the Tropical Western Pacific (TWP) site, located at 0.5°S and 166.9°E. The use of these parameterizations is suitable for models with a prognostic scheme for cloud mass content, but without explicit prediction of other moments of the ice crystal distribution.

The sensitivities of modeled radiative fluxes and cloud fields to the representation of r_e are investigated by incorporating the new scheme into the Scripps single-column model (SCM). Monte Carlo simulations determine how uncertainties in the r_e parameterizations scale up to give uncertainties in

modeled CRFs. Section 2 describes the development of the new parameterization and the associated uncertainties, Section 3 describes the simulations, and Section 4 discusses the significance of these findings.

Parameterizations of Microphysics for Tropical Cirrus

The microphysical parameterizations used in this study involve diagnostic relationships for r_e in terms of IWC and temperature. Following Fu (1996), it is assumed that

$$r_e = \frac{\sqrt{3}IWC}{\rho_i A_c} \quad (1)$$

where ρ_i is the density of ice. This definition is compatible with the single-scattering radiative parameterizations used in this study because modifications to Ebert and Curry's (1992) radiative scheme, based on this definition, are used (McFarquhar et al. 2002).

Habit-dependent size distributions for crystals with melted equivalent diameters, D_m , greater than 100 μm are derived by applying McFarquhar et al.'s (1999) neural network classification scheme to images recorded by a two-dimensional cloud probe (2DC). The numbers and sizes of smaller crystals, henceforth defined as crystals with D_m smaller than 100 μm , are determined using McFarquhar and Heymsfield 1997's parameterization scheme with coefficients randomly chosen from the surface of equally realizable solutions defined by McFarquhar et al. 2002. Ninety per cent of the 11633 small crystals used to develop the small crystal parameterization scheme were manually identified as spherical or quasi-spherical; however, Figures 22 and 23 of McFarquhar and Heymsfield (1996) show that many small crystals are not exactly spherical in shape. Therefore, their shape is represented using eighth order Chebyshev polynomials with coefficients chosen so that the projected areas of the Chebyshev particles equal those of the observed particles.

Figure 1 shows r_e , calculated using the size distributions defined above, as a function of IWC. There is no statistically significant dependence on temperature. The large scatter in the data occurs due to the stochastic application of the small crystal parameterization. The solid line represents the best fit of r_e as a function of IWC, obtained by applying matrix inversion to mean r_e values within a number of IWC bins, where

$$r_e = 10^{a+b\log(z)+c(\log z)^2} \quad (2)$$

with $z = IWC/IWC_0$, $IWC_0 = 1.0 \text{ g m}^{-3}$, and a , b , and c are coefficients of the fit. The thin dashed lines represent fits obtained for data points one and two standard deviations greater than or less than the mean r_e for each IWC.

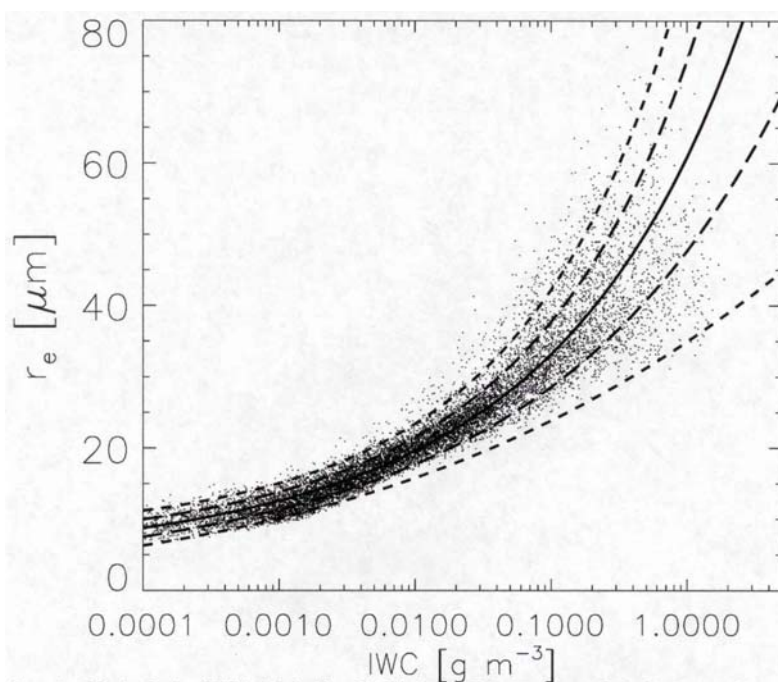


Figure 1. r_e defined as function of IWC, both derived from Central Equatorial Pacific Experiment (CEPEX) in situ data. Each dot represents 10 s (or 2 km) averaged size distribution. The solid line represents best fit to data, long dashed and short dashed lines represent fits for r_e greater than and less than one and two standard deviations from mean.

Other uncertainties in the derivation of Eq. (2) are assumptions about the number, masses, and size distributions of small ice crystals. Although the stochastic application of parameterizations somewhat accounts for these uncertainties, it must be acknowledged that the McFarquhar and Heymsfield 1997 was based on a limited set of data and that no measurements of small crystals were obtained for IWCs greater than 0.1 g m^{-3} . To investigate uncertainties associated with extrapolating the measured results to IWCs greater than 0.1 g m^{-3} , a sensitivity study is conducted where the mass in small crystals is set equal to that value estimated by assuming the total IWC is 0.1 g m^{-3} in Eq. (5) of McFarquhar and Heymsfield 1997; this should provide an upper bound on r_e by minimizing contributions of small crystals. The data are different from those in Figure 1 only for IWCs greater than 0.1 g m^{-3} . However, for IWCs between 0.5 and 1.0 g m^{-3} , the differences are substantial with a mean r_e of $63.1 \text{ }\mu\text{m}$ for the scheme minimizing small crystals compared to $46.0 \text{ }\mu\text{m}$ for the base scheme.

Alternately, the contributions of small crystals were maximized by using the size distributions measured by a forward scattering spectrometer probe (FSSP) installed on the same aircraft as the 2DC; FSSP measurements may be unreliable in ice clouds with substantial numbers of large ice crystals, but are useful in that they represent an upper bound for small crystal numbers (McFarquhar et al. 2002). The estimated r_e are much smaller, with mean values of 26.1 and $31.1 \text{ }\mu\text{m}$ for IWCs between 0.1 and 0.2 g m^{-3} and between 0.2 and 0.5 g m^{-3} respectively, compared to 37.2 and $46.0 \text{ }\mu\text{m}$ for the base case.

Although in situ measurements provide direct measurements of crystal size and shape, they are limited in that only one part of one cloud can be sampled at any time. Further, during a single field campaign only certain types of clouds in specific geographic regions are sampled. The observations used to construct Figure 1 were all collected in anvils associated with deep convection in the Tropics.

Therefore, these in situ data are supplemented with cirrus layer microphysical properties derived from MMCR and AERI data, by applying Mace et al.'s (1998) algorithm to measurements collected during June and July of 1999 at Nauru Island. Three minute means of layer mean IWC and layer mean r_e were retrieved every 8 minutes provided that there were no intervening clouds. Because only optically thin layers produce reasonable results at this time, the data were quality controlled so that clouds with emittances greater than 0.85 were excluded from the sample.

Figure 2 plots r_e as a function of IWC for the layer mean averages. Solid lines represent best fits to the data, and the long and short dashed lines represent fits for one and two standard deviations above and below the mean. As before, the cirrus were sampled under conditions of IWCs lower than 0.1 g m^{-3} , so extrapolations of the curves beyond this point are uncertain. When comparing against the in situ data in Figure 1, the r_e from the remote sensing method are higher than those observed in situ. For example, for IWCs between 0.005 and 0.01 g m^{-3} and between $.05$ and 0.1 g m^{-3} , the in situ r_e medians are 18.7 and $30.7 \text{ }\mu\text{m}$, whereas the remotely sensed r_e medians are 44.6 and $73.9 \text{ }\mu\text{m}$. For mid-latitude cirrus, Mace et al. (2001) showed that larger r_e and IWCs typically occur for thicker clouds. Since the CEPEX measurements were probably biased somewhat towards the tops of clouds (McFarquhar and Heymsfield 1997), and since r_e typically decreases with increasing altitude in cirrus, these point measurements may be expected to be somewhat lower than layer averages. The addition of small crystals to data from standard optical array probes also lowers the in situ r_e values.

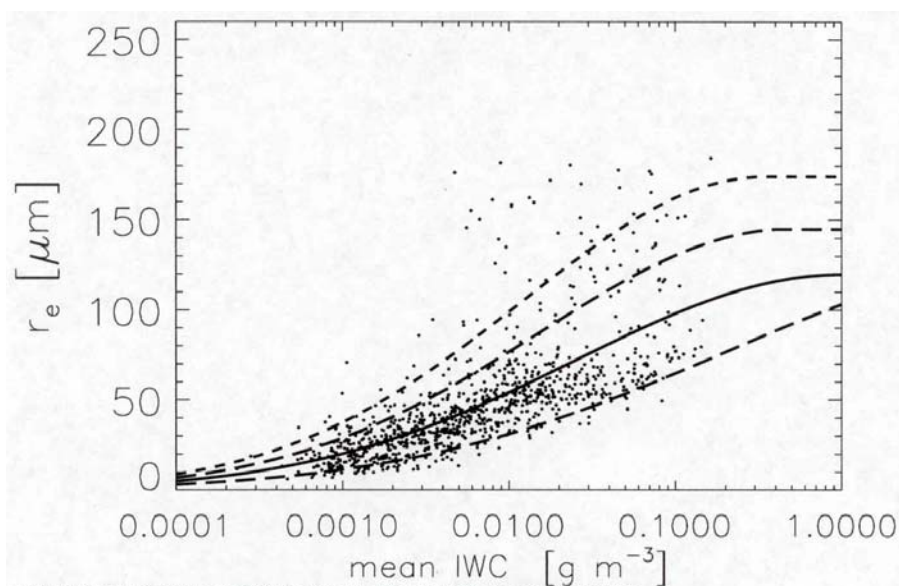


Figure 2. As in Figure 1, except r_e and IWC obtained from retrievals based on remotely sensed data.

Modeling Studies

The model used in this study is the SCM described by Iacobellis and Somerville (2000). Following their study of tropical clouds for the Tropical Ocean Global Atmosphere-Coupled Ocean Atmosphere Response Experiment (TOGA-COARE) time period, we use a time step of 7.5 min, an ocean surface albedo of 0.05, and a diurnally varying solar signal dependent on latitude and time of the year. The relaxed Arakawa-Schubert cumulus convection scheme is used, and maximum overlap of clouds is assumed. A vertical resolution of 53 layers is used because the finer resolution allows more details of the microphysical-radiative interactions to be resolved. All nonspecified options follow those used by Iacobellis and Somerville (2000).

Simulations describe, and are based upon, conditions measured at the Atmospheric Radiation Measurement (ARM) Program's TWP site, located in the area between 10°N to 10°S from Indonesia to near Christmas Island in the warm pool region. The period August 9, 2000 through September 8, 2000, is chosen for simulation because data collected by the MMCR at Nauru Island (167°E, 2°S) indicated that there was moderated cirrus activity during this time. Further, SCM simulations conducted over the entire second half of 2000 and the entire 2001 time frame indicated that high cloud cover and high cloud optical depth were near a maximum for this time period. The forcing data were derived from the National Centers for Environmental Prediction (NCEP)'s global spectral model (GSM). Since these data are from a forcing model, rather than from observations, the forcing might not be as accurate as for typical SCM simulations; however, preliminary indications are that the SCM performs adequately.

Both fully interactive and non-interactive simulations are performed to represent conditions observed at the ARM TWP site. With fully interactive microphysics, ice and cloud water path vary according to the prognostic equations used in the model (e.g., Tiedtke 1993); differences in microphysical properties produce changes in heating profiles, which in turn alter ice and cloud water amounts. Small variations in IWC produced by different schemes quickly amplify so that differences in parameterization schemes are quickly dominated by differences in IWC. In non-interactive simulations, ice and cloud water path are forced to that value predicted by a base simulation; differences in heating rates do not feedback upon ice and cloud water amounts. The first studies determine net uncertainties associated with the parameterization schemes, whereas the second studies help better understand factors causing variations in modeled properties.

A series of simulations are run, corresponding to different fit coefficients for Eq. (1) describing both the in situ and remotely sensed data (base coefficients and coefficients corresponding to r_e one and two standard deviations greater than and less than base conditions). Simulations corresponding to maximizing and minimizing concentrations of small crystals are also performed, as is a simulation with a constant r_e of 10 μm . Shortwave (SW) and longwave (LW) CRFs at the surface and at top of the atmosphere (TOA) are derived for the fully interactive simulations describing these conditions. Variations in LW CRF at the TOA and at the surface are similar, with maximum differences of 6.4 W m^{-2} and 6.3 W m^{-2} between simulations. Variations in SW CRF are much larger, with a difference of 34.2 W m^{-2} between the constant 10 μm simulation and the simulation with r_e 2 σ higher than the mean value. Further, the difference between simulations with r_e 2 σ greater than and less than the base r_e is 17.7 W m^{-2} .

Figure 3 illustrates the variation of SW and LW CRF at TOA and of cloud cover and precipitation as a function of time for the fully interactive simulations. Figure 4 plots the average ice water paths (IWP), liquid water paths (LWP), liquid (τ_l) and ice (τ_i) optical depths, and cloud averaged ice and liquid r_e as a function of time. The average IWP and LWP for these simulations are 131 and 162 g m^{-2} , respectively. Differences in τ_l can be considerable at certain times (e.g., August 15 and August 22). A large difference in τ_l or τ_i alone may not indicate a large difference in CRF. For example, the TOA SW CRF

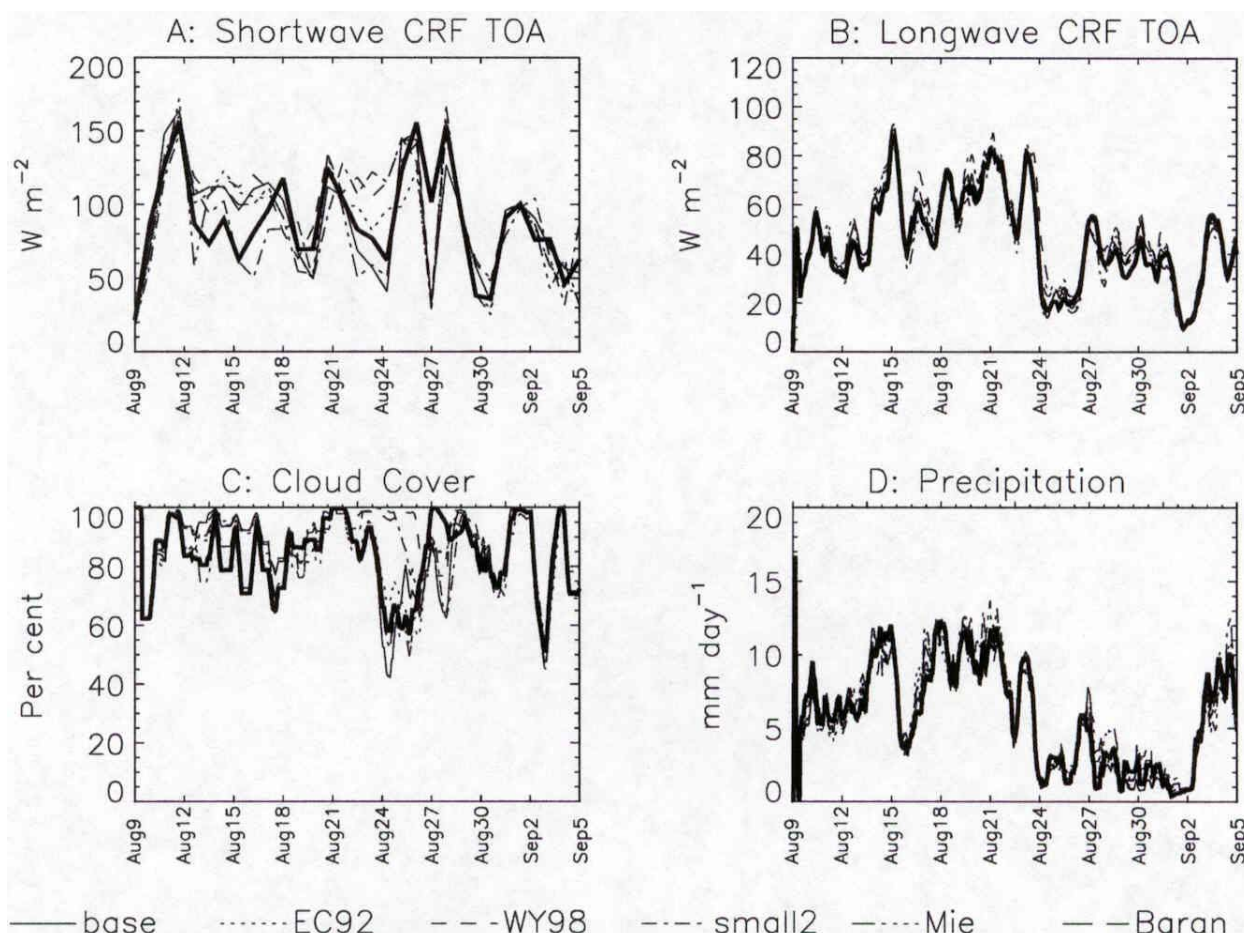


Figure 3. Temporal variation of SW CRF at TOA, LW CRF at TOA, cloud cover, and precipitation for 35-day simulation of conditions at the ARM TWP site. The different line types represent simulations indicated in legend. The thick line represents simulation with constant r_e of 10 μm .

does not differ substantially between simulations around August 21; LWP from the 10 μm simulation is much larger than LWP from the base simulation, but a smaller IWP compensates. In general, though, larger differences in IWP or LWP are associated with larger differences in SW CRF. Differences in these quantities were also examined for the non-interactive simulations (figures not shown). Similar trends were noted, but the magnitude of differences between simulations is typically reduced.

McFarquhar et al. 2002 describes these comparisons in more detail. In summary, variations in LWP and IWP between simulations occur because the variation in r_e causes changes in the cloud water prognostic equations, which feedback upon IWP and LWP.

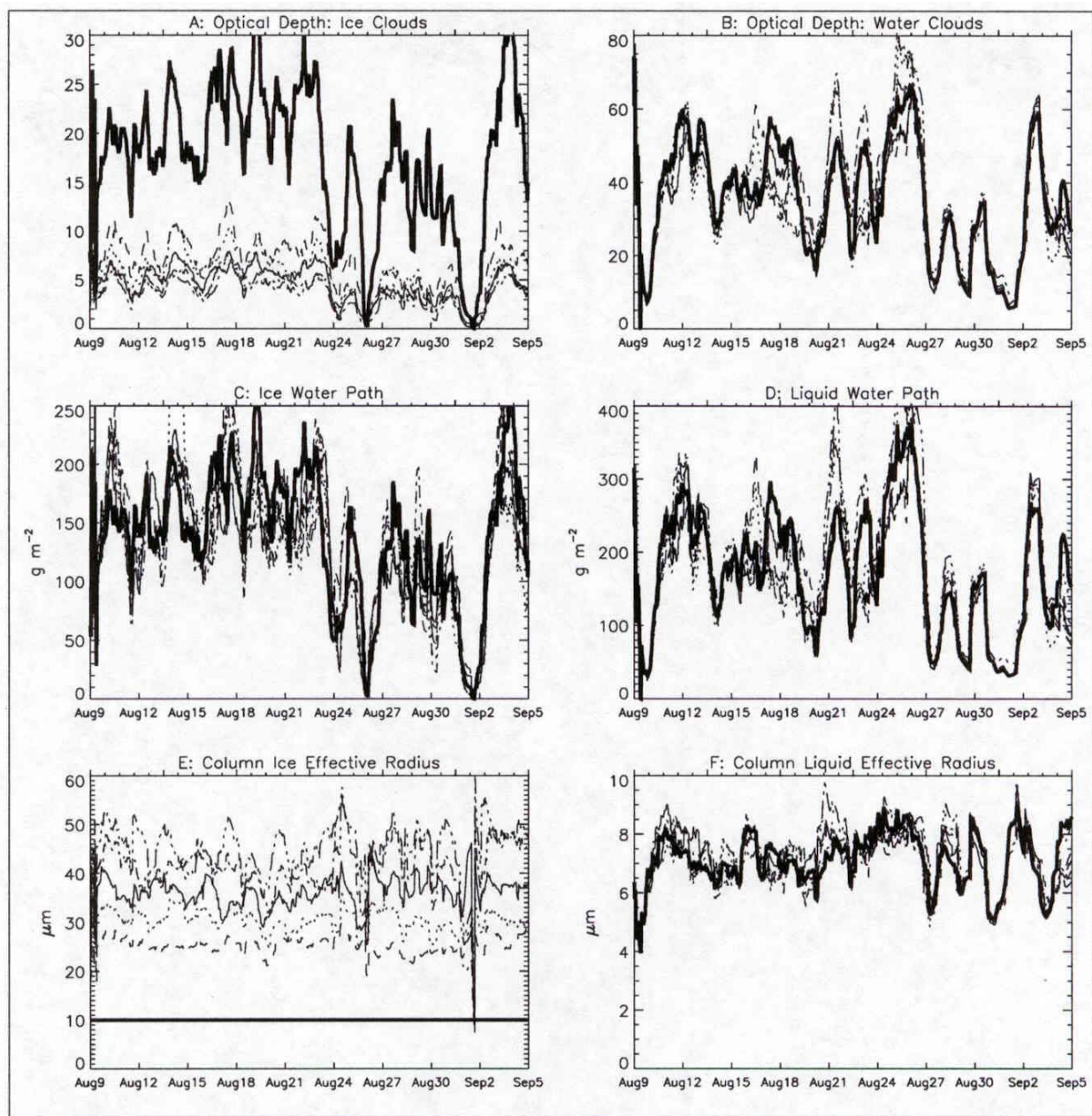


Figure 4. As in Figure 3, except for temporal variation of τ_i , τ_l , IWP, LWP, and average r_e for ice and liquid clouds. Thick line represents simulation with constant r_e of 10 μm .

To understand why CRFs vary between simulations, the 10 μm simulation is compared in detail against the simulation where r_e is characterized by the base conditions of Figure 1. Figure 5 shows the time-averaged vertical profiles of CMC, r_e , cloud fraction and cloud extinction as a function of height for these two simulations. Two lines are plotted for r_e , corresponding to liquid and ice particles, with the overlap representing mixed-phase. The extinction of upper clouds for the base simulation are substantially less than for the 10 μm simulation because of larger r_e . However, substantial differences in

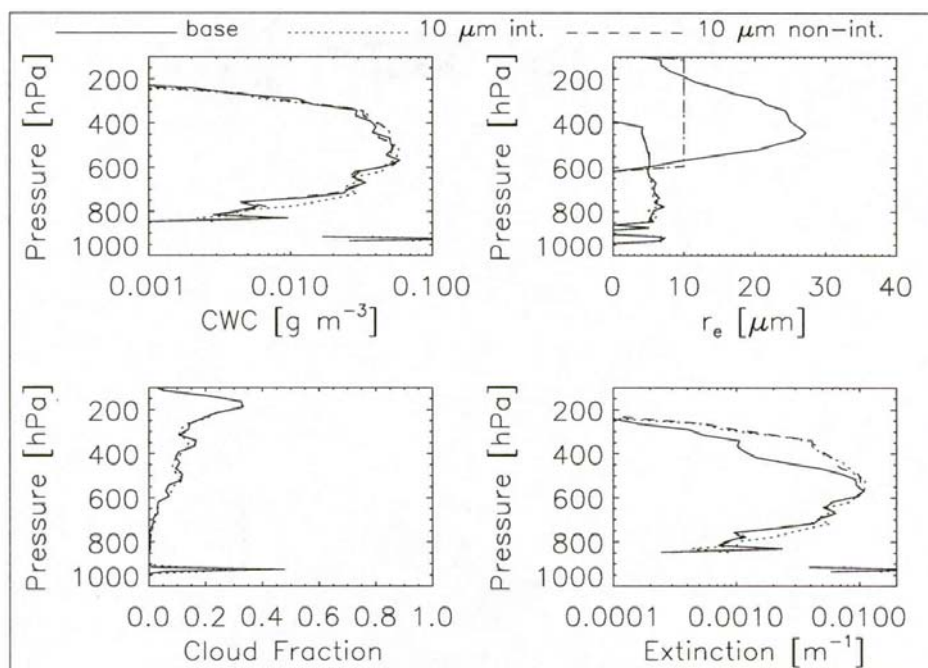


Figure 5. Vertical profile of CWC, r_e , cloud fraction, and extinction averaged over 35-day period of ARM TWP simulation. Line types correspond to simulations indicated in legend.

LWCs also exist when the interactive simulations are compared. The base simulation has substantially higher LWCs and extinction optical depths around 825 hPa and substantially lower LWCs around 750 hPa.

Other sensitivity studies examined the impact of randomly choosing parameterization coefficients in Eq. (2) at each model timestep. Because the scatter in Figure 1 cannot be adequately understood or parameterized at this time, it needs to be accounted for in a statistical manner in the application of parameterizations to reproduce the observed variability. When Monte Carlo simulations are conducted where r_e is randomly chosen to be within 1 or 2 σ of the most likely r_e at each timestep, the SW CRF at the TOA and surface can vary by up to 13.3 W m^{-2} and 11.2 W m^{-2} , respectively, between simulations; for LW CRF, differences of 2.4 W m^{-2} at the surface and 4.5 W m^{-2} at TOA are noted. The Monte Carlo simulations typically involve an enhancement of SW reflection compared to the base simulations (8 out of 12 simulations give enhanced reflections), and there is no reason to expect that the average of a series of such simulations should equal the simulation from the average parameterization because of inherent non-linear interactions between radiation and microphysics.

A final sensitivity study examined the sensitivity of simulations to the parameterization developed with the remote sensing observations. Because the retrieved r_e are larger than those observed in situ, the amount of SW reflection, and hence the SW CRF, is reduced (by 7.4 W m^{-2} for and by 18.3 W m^{-2} for the extremely large estimated r_e compared to the base cases). Even larger differences are noted when compared to some of the smaller r_e estimated from the in situ parameterizations that assumed larger concentrations of small crystals.

Discussion and Summary

Using in situ measurements of the sizes and shapes of ice crystals and using retrievals from a combination of radar/interferometer data, a new parameterization describing the dependence of r_e , on cloud IWC has been developed. It extends previous schemes in that it accounts for the numbers, sizes, and shapes of small ice crystals, with diameters smaller than 100 μm , and provides information about the range of variance of r_e for a given IWC, which is important given that observed r_e values vary substantially for a given IWC and temperature. In addition, there are large uncertainties in the representation of r_e due to uncertainties in typical sizes, shapes, and numbers of small crystals.

The use of the parameterization is suitable for large-scale models with a prognostic scheme for cloud water, but without explicit prediction of other moments of the size distribution. The parameterization can be used for the simulation of tropical environments where cirrus clouds are generated by deep convection; it is not known how readily it can be extended to other geographical regimes and clouds produced by other formation mechanisms.

The parameterization was implemented in the Scripps SCM, and simulations describing the ARM TWP site were conducted. Sensitivity studies determined how uncertainties in the parameterization scheme scaled up to predicted uncertainties in CRF. Observational uncertainties in the prediction of r_e , when represented in the model, can cause differences of up to 25 W m^{-2} in predicted SW CRF. Monte Carlo simulations were used to show that the mean of a series of simulations is not necessarily the same as a simulation of the mean conditions, with an enhanced reflection of shortwave radiation typically observed. The mechanisms by which different parameterizations impact CRF were examined by comparing the base simulation with a simulation assuming a constant r_e of 10 μm . The effect of different microphysical and radiative properties on LW heating rates ultimately caused the differences. Both fully interactive simulations, where changes in heating rates associated with different microphysical parameterizations feedback upon the cloud water content prognosed, and non-interactive simulations, where such feedbacks are not allowed, were used to better describe the feedbacks occurring.

Future studies should concentrate on extending this analysis to other cloud types forming in different geographic regimes due to different cloud formation mechanisms. Further, parameterizations of r_e in terms of IWC only and temperature may not be adequate; other synoptic variables could also be added into the parameterization development.

Acknowledgments

This research was supported by the U.S. Department of Energy's (DOE's) ARM Program under Contract Numbers DE-FG03-00ER62913 and DE-FG03-97ER62338. Data were obtained from the ARM Program sponsored by the U.S. Department of Energy, Office of Science, Office of Biological and Environmental Research, Environmental Sciences Division. The assistance of Michael Timlin in figure preparation is acknowledged.

Corresponding Author

Dr. Greg M. McFarquhar, mcfarq@atmos.uiuc.edu, (217) 265-5458

References

Ebert, E. E., and J. A. Curry, 1992: A parameterization of ice cloud optical properties for climate models. *J. Geophys. Res.*, **97**, 3831-3836.

Fu, Q., 1996: An accurate parameterization of the solar radiative properties of cirrus clouds. *J. Climate*, **9**, 2058-2082

Iacobellis, S. F., and R. C. J. Somerville, 2000: Implications of microphysics for cloud-radiation parameterizations: lessons from TOGA-COARE. *J. Atmos. Sci.*, **57**, 161-183.

Mace, G. G., T. P. Ackerman, P. Minnis, and D. F. Young, 1998: Cirrus layer microphysical properties derived from surface-based millimeter radar and infrared interferometer data. *J. Geophys. Res.*, **103**, 23,207-23,216.

Mace, G. G., E. E. Clothiaux, and T. P. Ackerman, 2001: The composite characteristics of cirrus clouds: Bulk properties revealed by one year of continuous cloud radar data. *J. Climate*, **14**, 2185-2203.

McFarquhar, G. M., and A. J. Heymsfield, 1996:

McFarquhar, G. M., and A. J. Heymsfield, 1997: Parameterization of tropical cirrus ice crystal spectra and implications for radiative transfer: Results from CEPEX. *J. Atmos. Sci.*, **54**, 2187-2201.

McFarquhar, G. M., A. J. Heymsfield, A. Macke, J. Iaquina, and S. M. Aulenbach, 1999: Use of observed ice crystal sizes and shapes to calculate mean scattering properties and multi-spectral radiances: CEPEX 4 April 1993 case study. *J. Geophys. Res.*, **104**, 31763-31779.

McFarquhar, G. M., S. F. Iacobellis, R. C. J. Somerville, G. G. Mace, and Y. Zhang, 2002: Impacts of cloud microphysics on modeled cloud and radiative properties: SCM simulations. *J. Climate*, submitted.

Petch, J. C., 1998: Improved radiative transfer calculations from information provided by bulk microphysical schemes. *J. Atmos. Sci.*, **49**, 1846-1858.

Tiedtke, M., 1993: Representation of clouds in large-scale models. *Mon. Wea. Rev.*, **121**, 3040-3061.

Zhang, Y., A. Macke, and F. Albers, 1999: Effect of crystal size spectrum and crystal shape on stratiform cirrus radiative forcing. *Atmos. Res.*, **52**, 59-75.